

Supporting Information

All-in-one Fiber for Stretchable Fiber-Shaped Tandem Supercapacitors

Zhuanpei Wang^a, Jianli Cheng^{a*}, Qun Guan^a, Hui Huang^a, Yinchuan Li^a, Jingwen

Zhou^a, Wei Ni^a, Bin Wang^{a*}, Sisi He^b, Huisheng Peng^{b*}

^aInstitute of Chemical Materials, China Academy of Engineering Physics, Mianyang, Sichuan 621900, China; Email: jianlicheng@caep.cn, binwang@caep.cn

^bState Key Laboratory of Molecular Engineering of Polymers, Department of Macromolecular Science, and Laboratory of Advanced Materials, Fudan University, Shanghai 200438, China; Email: penghs@fudan.edu.cn.

* The corresponding author. jianlicheng@caep.cn, penghs@fudan.edu.cn, binwang@caep.cn.

1. Supporting Video

The wet-spinning process in preparing the PEDOT:PSS fiber (Movie S1). PEDOT:PSS precursor with certain concentration and viscosity was injected into a coagulating bath of calcium chloride and pretreated by solvents to form a PEDOT:PSS fiber.

2. Supporting figures

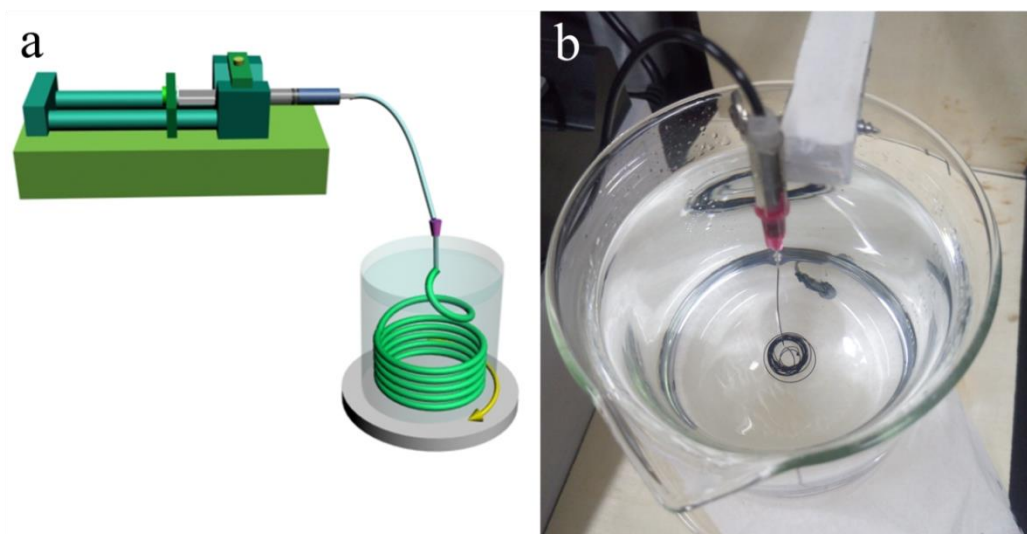


Figure S1. (a) Schematic illustration to the wet-spinning process of the PEDOT:PSS fiber. (b) Photograph of the wet-spinning process of the PEDOT:PSS fiber.

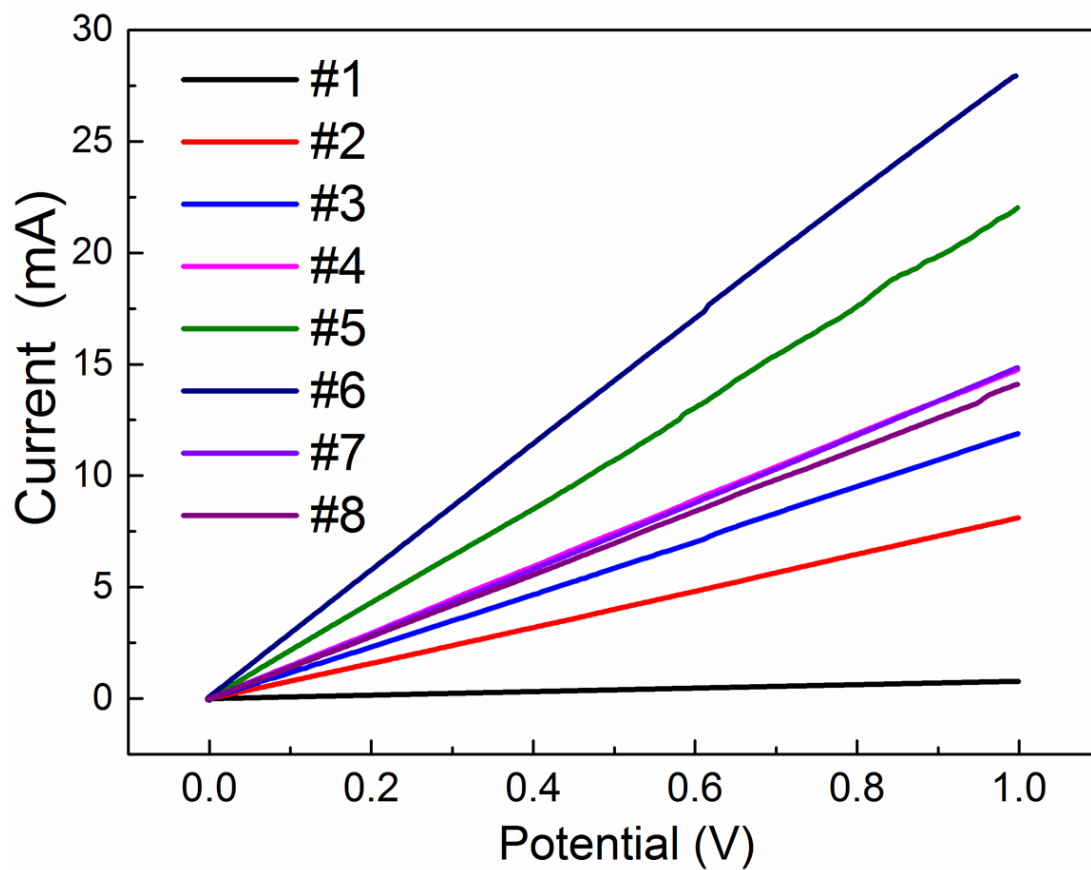


Figure S2. I-V curves of PEDOT:PSS and PEDOT-S:PSS fibers after different treating times of sulfuric acid and solvents (Sample PEDOT-S:PSS-#1 to 8).

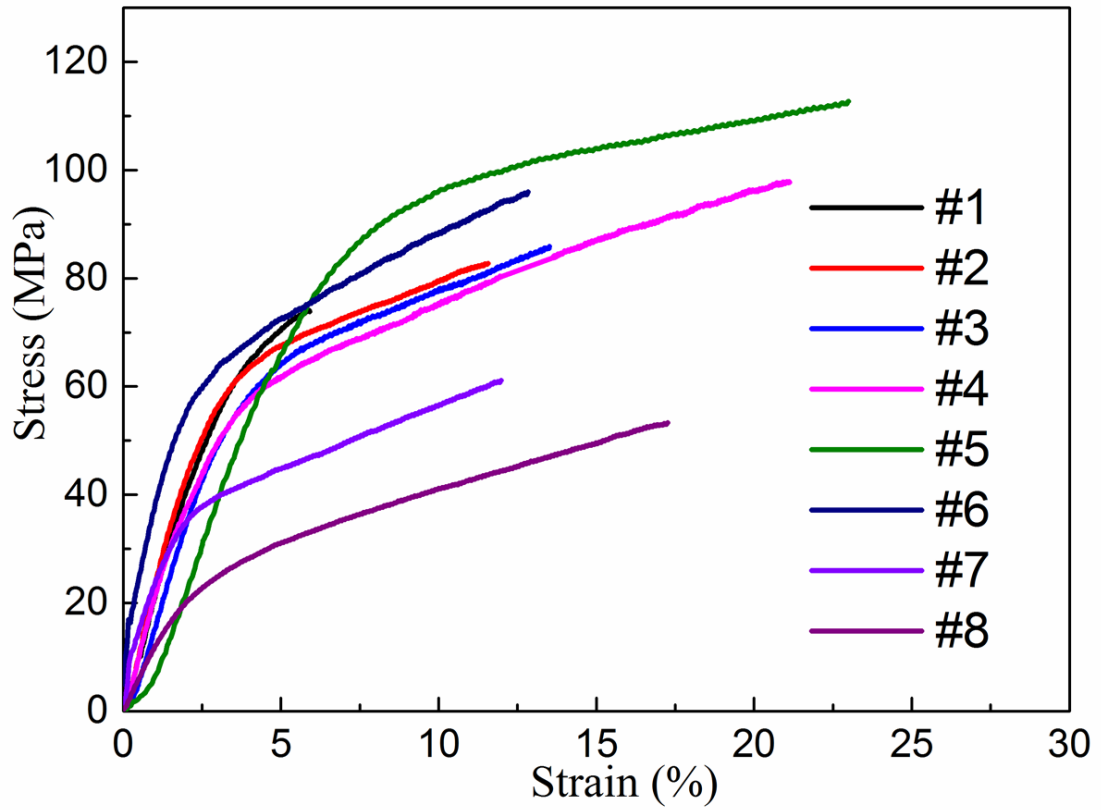


Figure S3. Strain-stress curves of PEDOT:PSS and PEDOT-S:PSS fibers after different treating times of sulfuric acid and solvents (Sample PEDOT-S:PSS-#1 to 8).

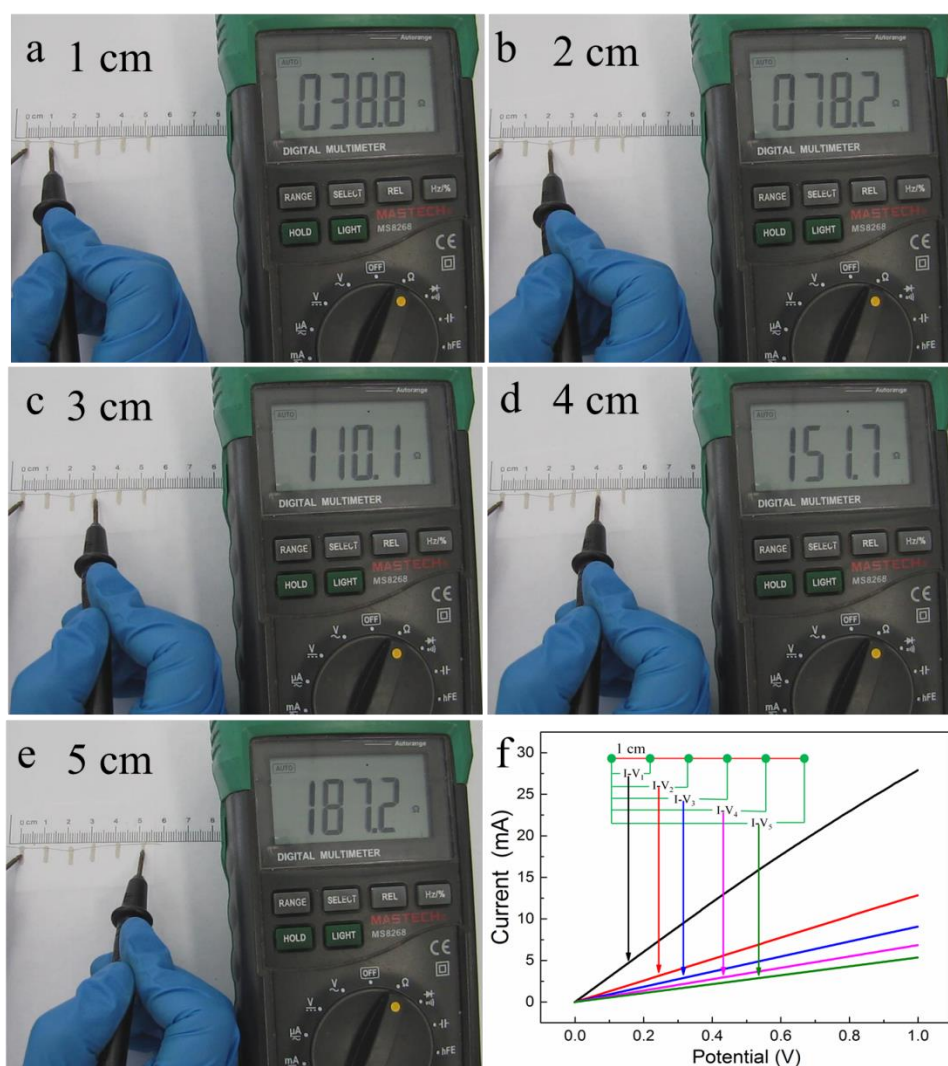


Figure S4. (a-e) The electrical resistance of PEDOT-S:PSS-#6 at different length obtained from the multimeters and (f) the I-V curves of PEDOT-S:PSS-#6 at different length obtained from electrochemical workstation.

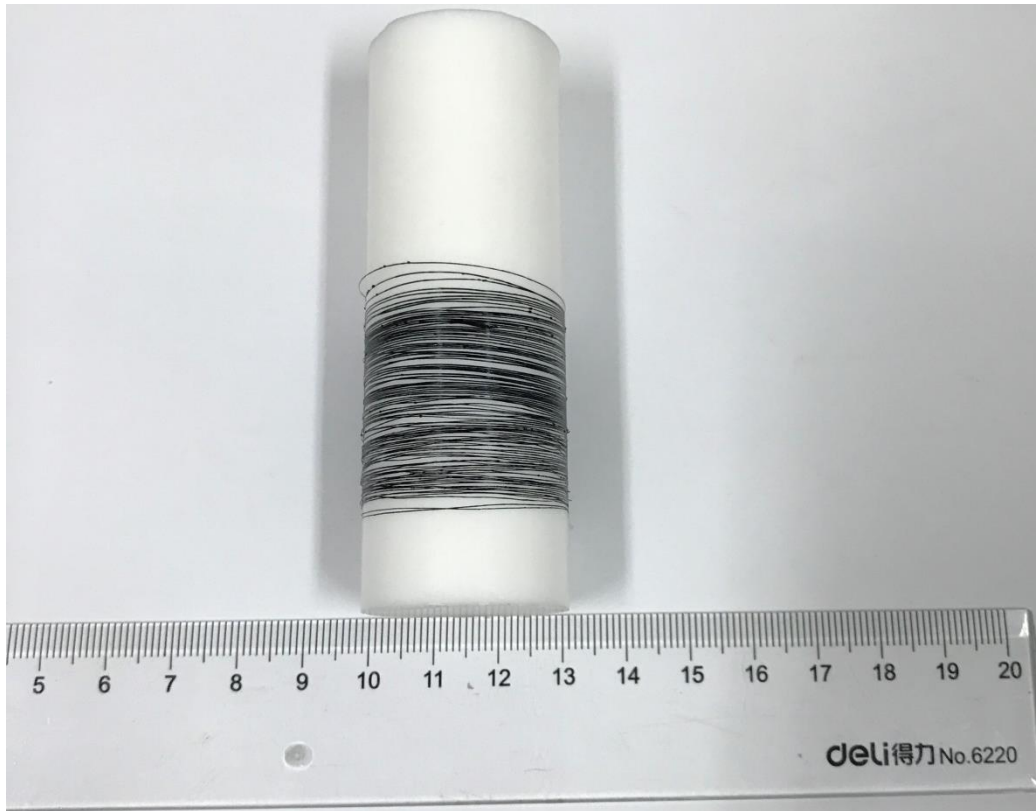


Figure S5. Photograph of a continuous PEDOT-S:PSS fiber with length of over 10 m wrapped on a PTFE rod. Scale bar, 1 cm.

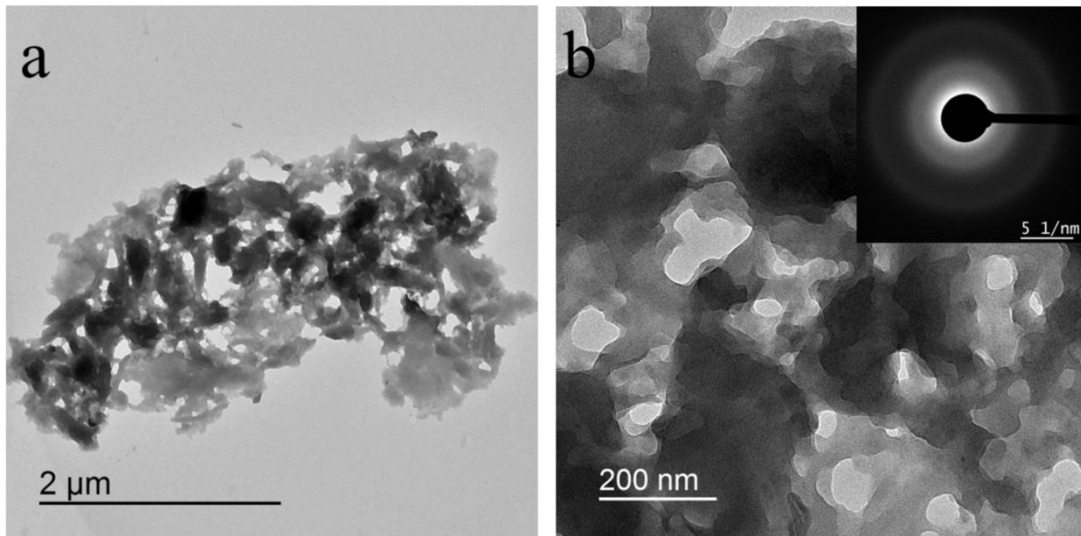


Figure S6. (a) TEM image of the cross-section part sliced from the PEDOT:PSS fiber electrode without sulfuric acid treatment. (b) High-magnification TEM image of PEDOT:PSS (the inset, selected area electron diffraction).

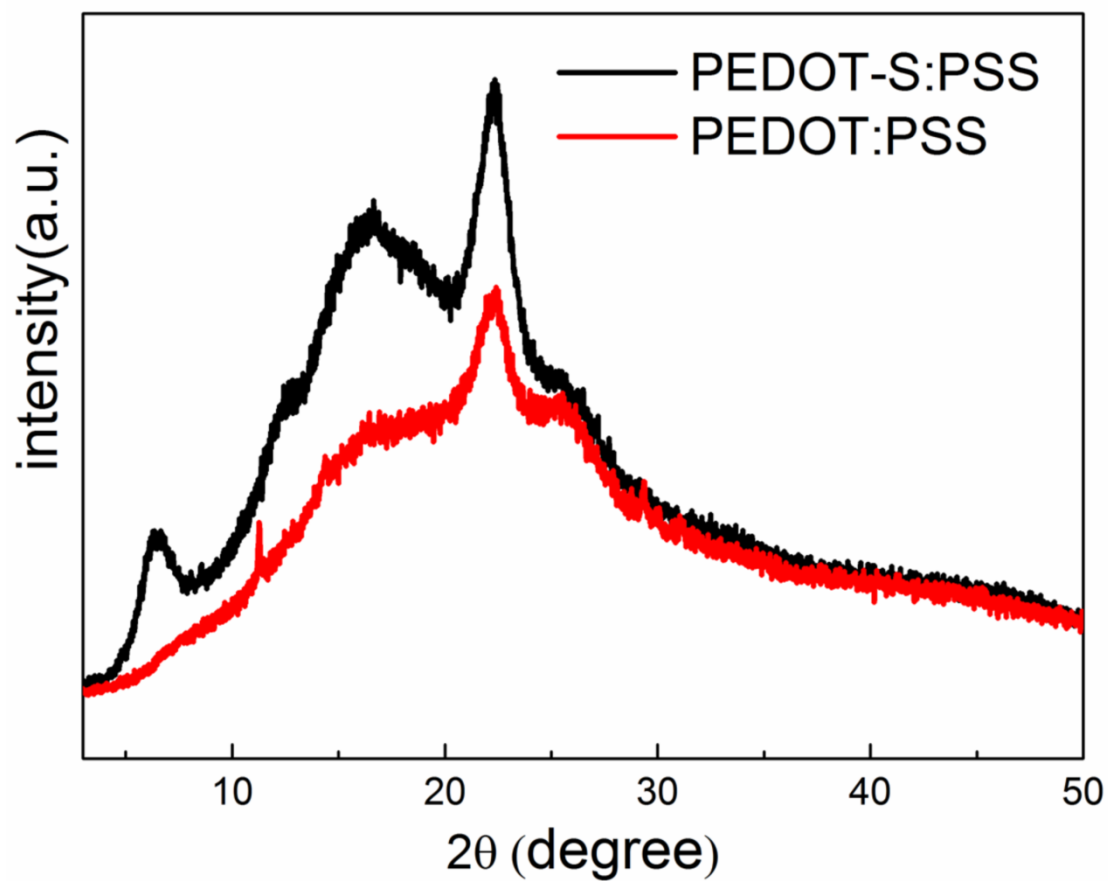


Figure S7. XRD patterns of PEDOT:PSS and PEDOT-S:PSS.

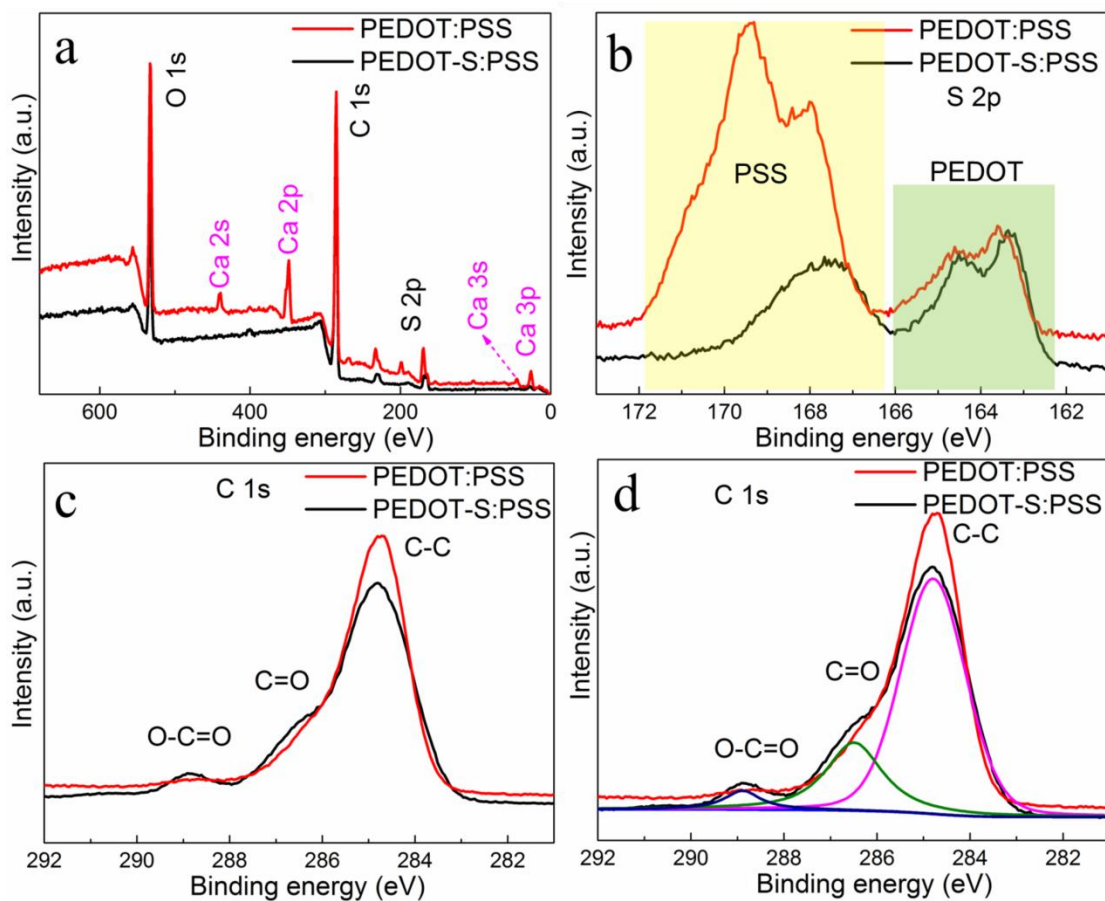


Figure S8. XPS spectra of PEDOT:PSS and PEDOT-S:PSS fiber. (a) Total elements, (b) S 2p, (c) C 1s and (d) C 1s of PEDOT-S:PSS fiber.

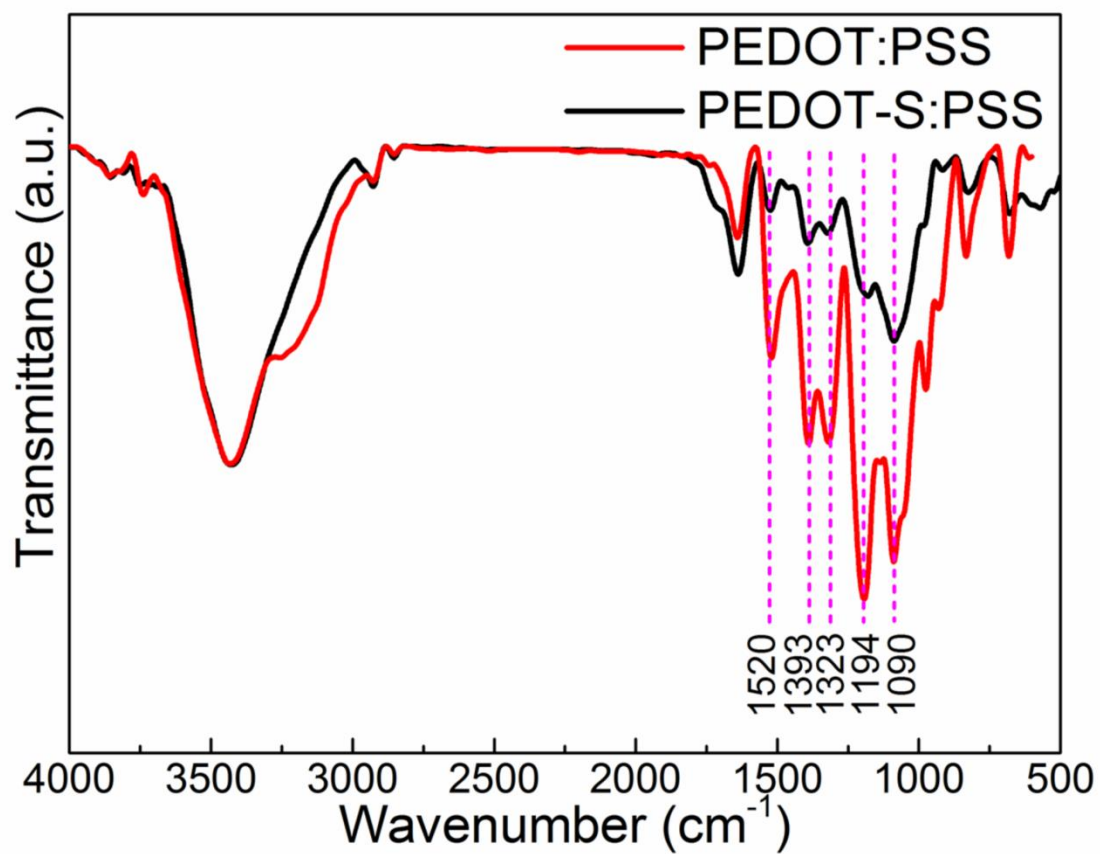


Figure S9. FT-IR spectra of PEDOT:PSS and PEDOT-S:PSS fibers.

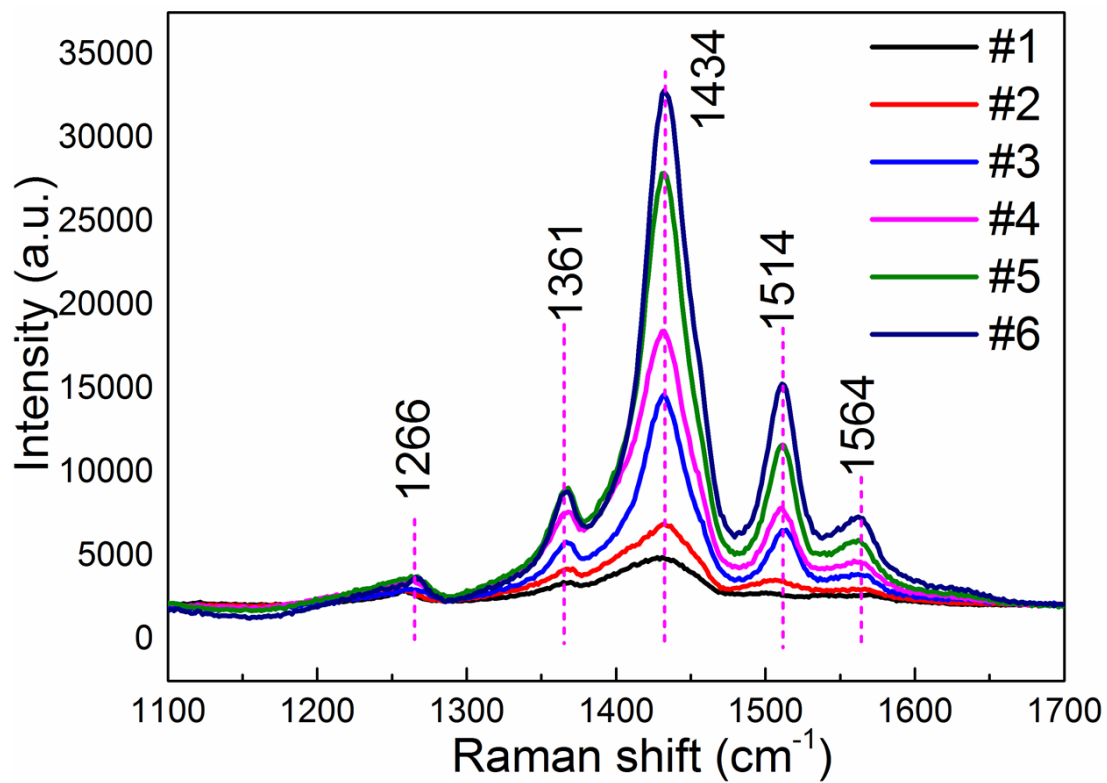


Figure S10. Raman spectra of PEDOT:PSS and PEDOT-S:PSS fibers after different treating times of sulfuric acid and solvents (Sample PEDOT-S:PSS-#1 to 6).

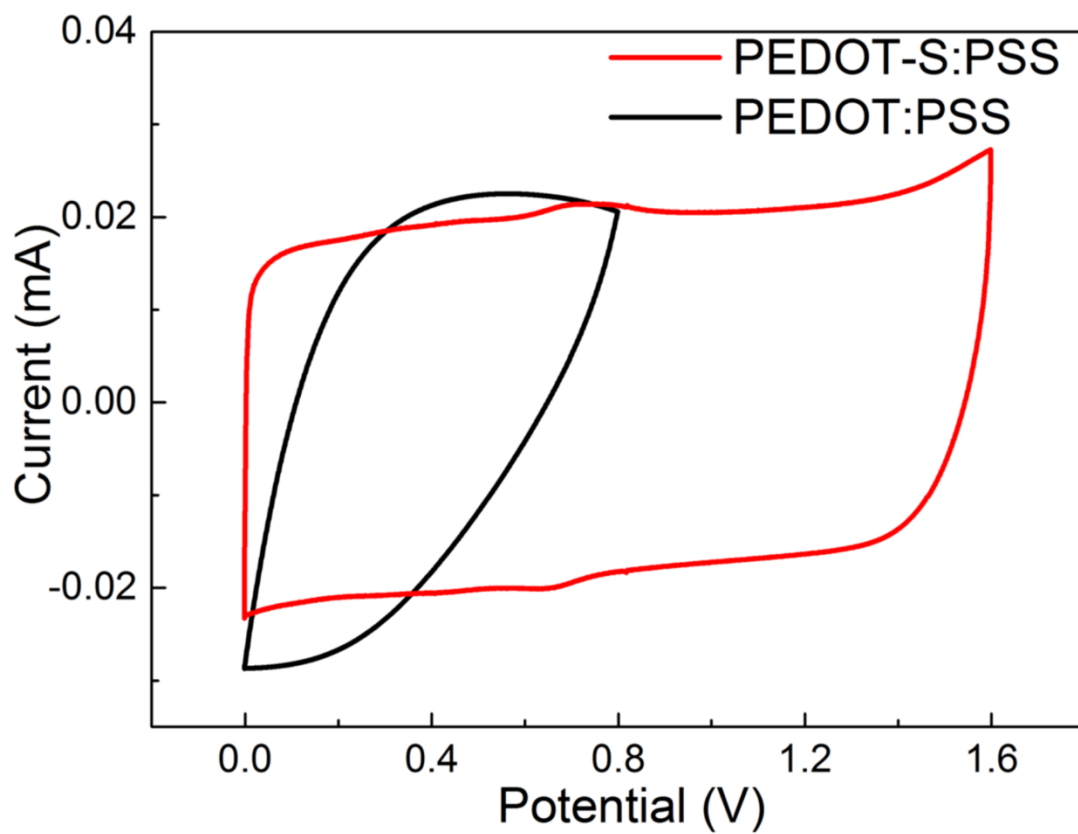


Figure S11. CV curves being obtained at potential ranges of 0 to 0.8 V and 0 to 1.6 V at a scan rate of 20 mV s^{-1} for PEDOT:PSS and PEDOT-S:PSS fiber, respectively.

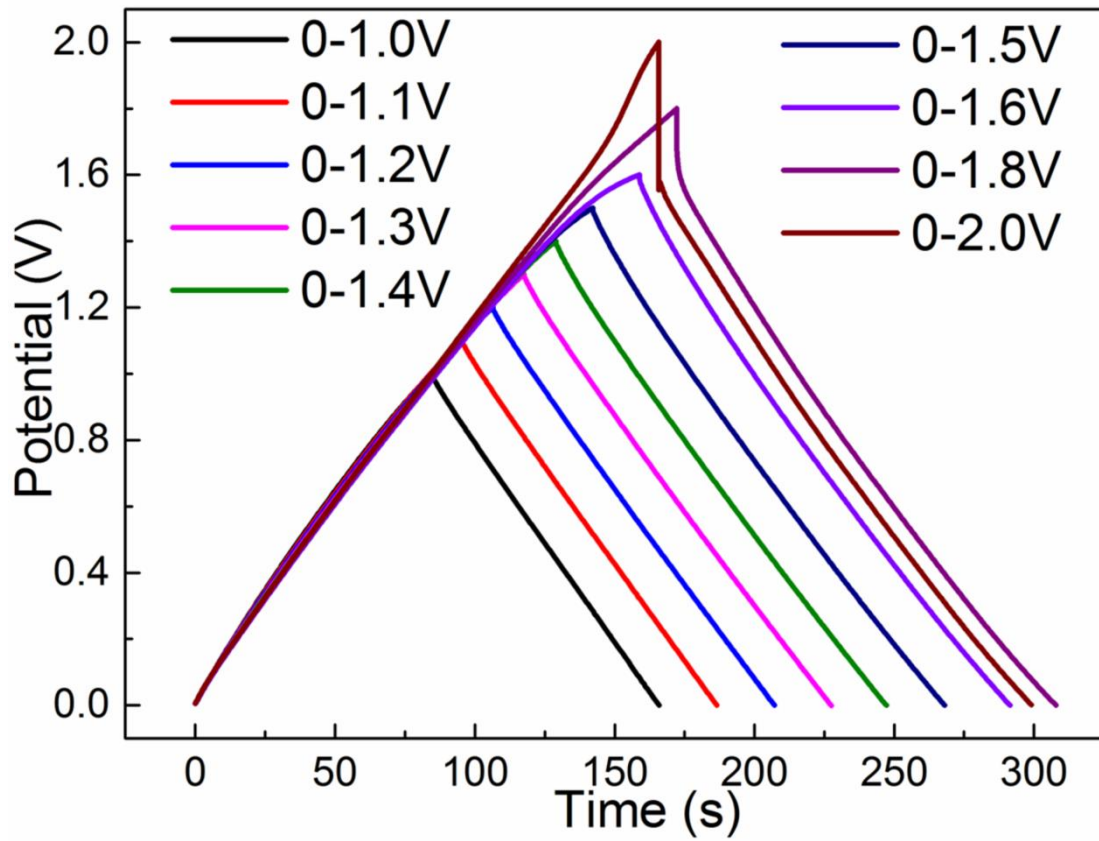


Figure S12. Galvanostatic charge-discharge curves for PEDOT-S:PSS fiber under different voltages at a current density of $500 \mu\text{A cm}^{-2}$.

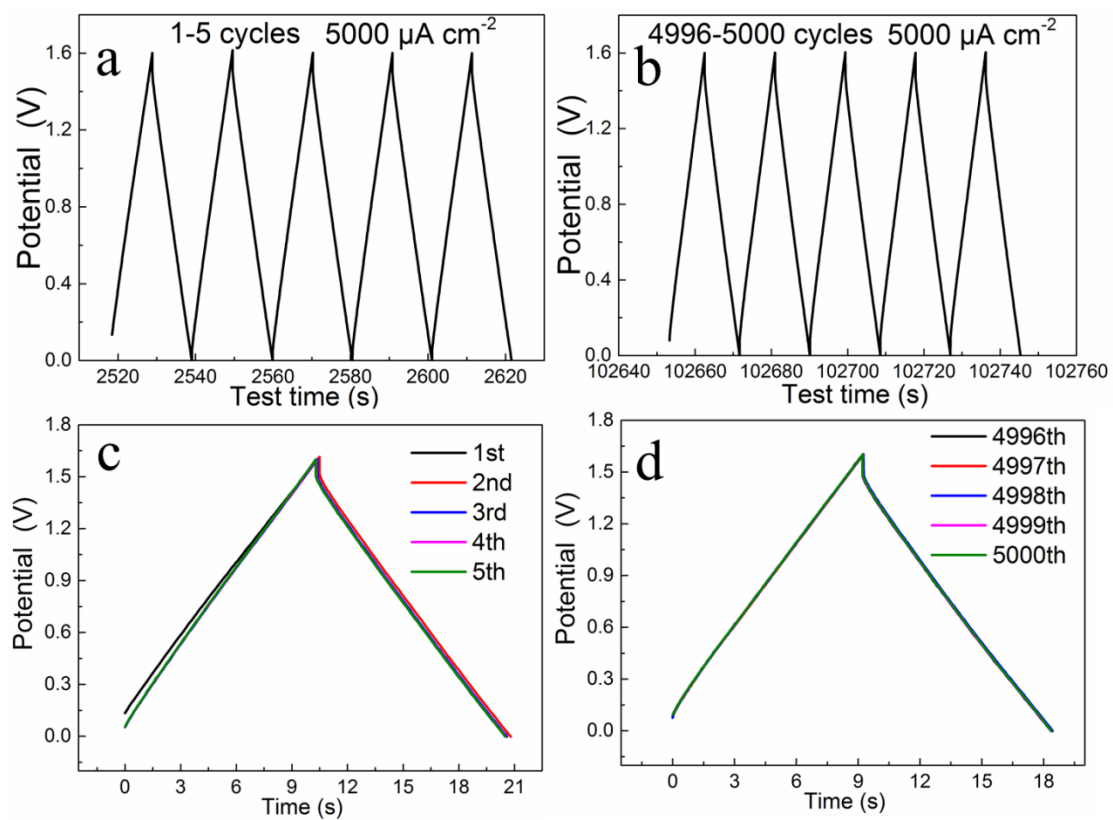


Figure S13. The galvanostatic charge-discharge curves of PEDOT-S:PSS fiber for (a, c) the first five and (b, d) the last five cycles.

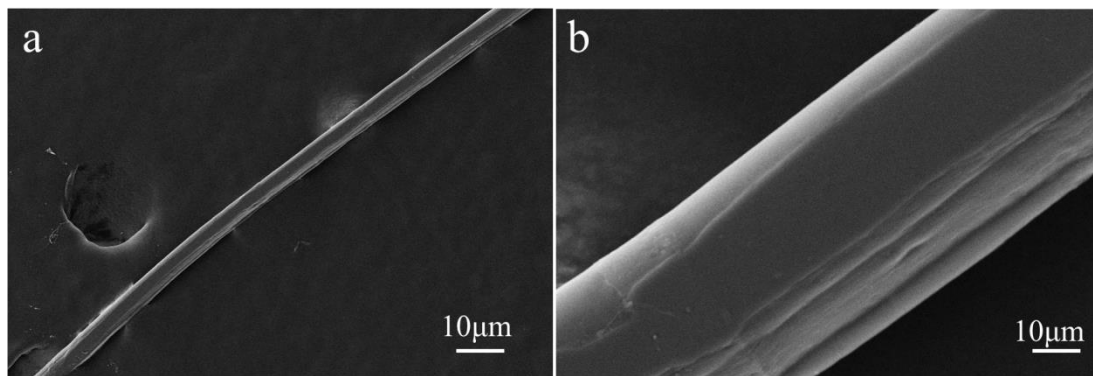


Figure S14. SEM images of PEDOT-S:PSS fiber after 5,000 charging-discharging cycles at $5,000 \mu\text{A cm}^{-2}$.

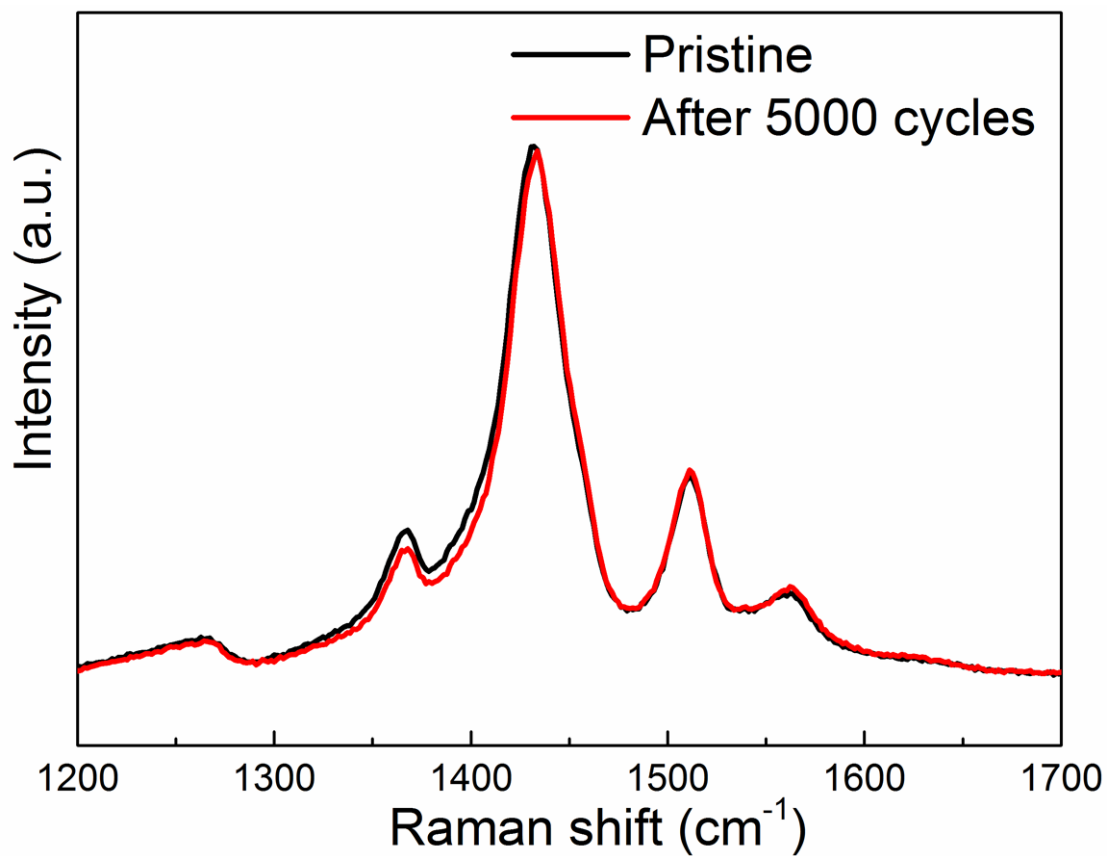


Figure S15. Raman spectra of PEDOT-S:PSS fiber before and after 5,000 charging-discharging cycles at 5,000 $\mu\text{A cm}^{-2}$.

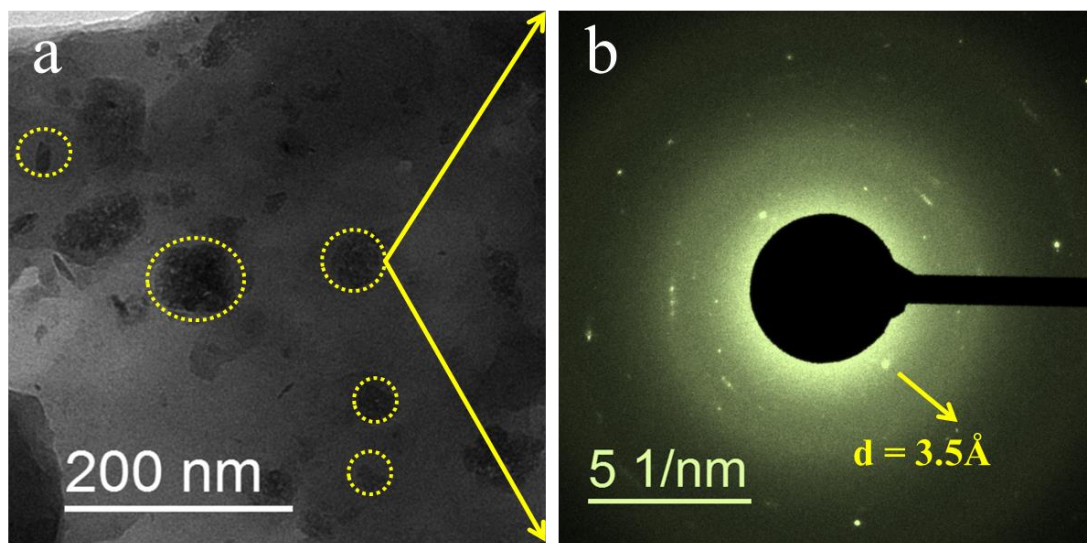


Figure S16. (a) TEM image and (b) SAED of PEDOT-S:PSS fiber after 5,000 charging-discharging cycles at $5,000 \mu\text{A cm}^{-2}$.

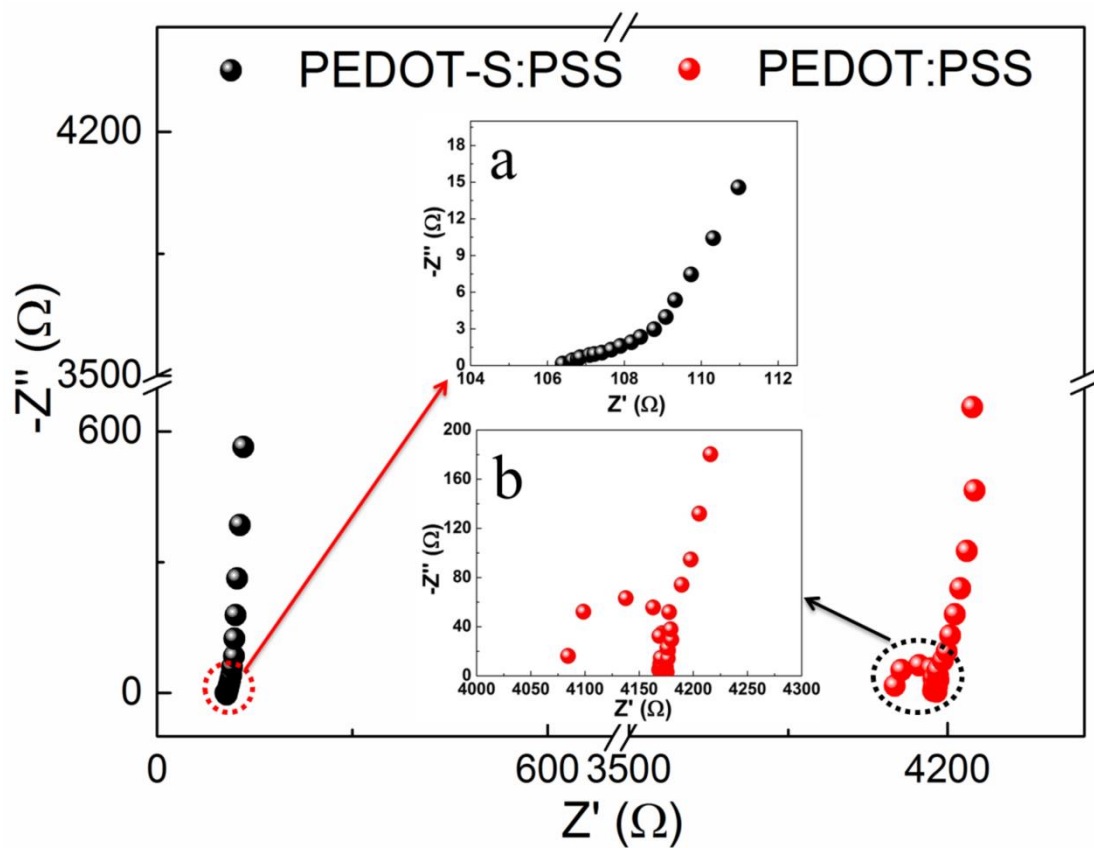


Figure S17. Electrochemical impedance spectroscopy of PEDOT-S:PSS and PEDOT:PSS fiber. The insets are (a) the magnified curves of PEDOT-S:PSS and (b) PEDOT:PSS.

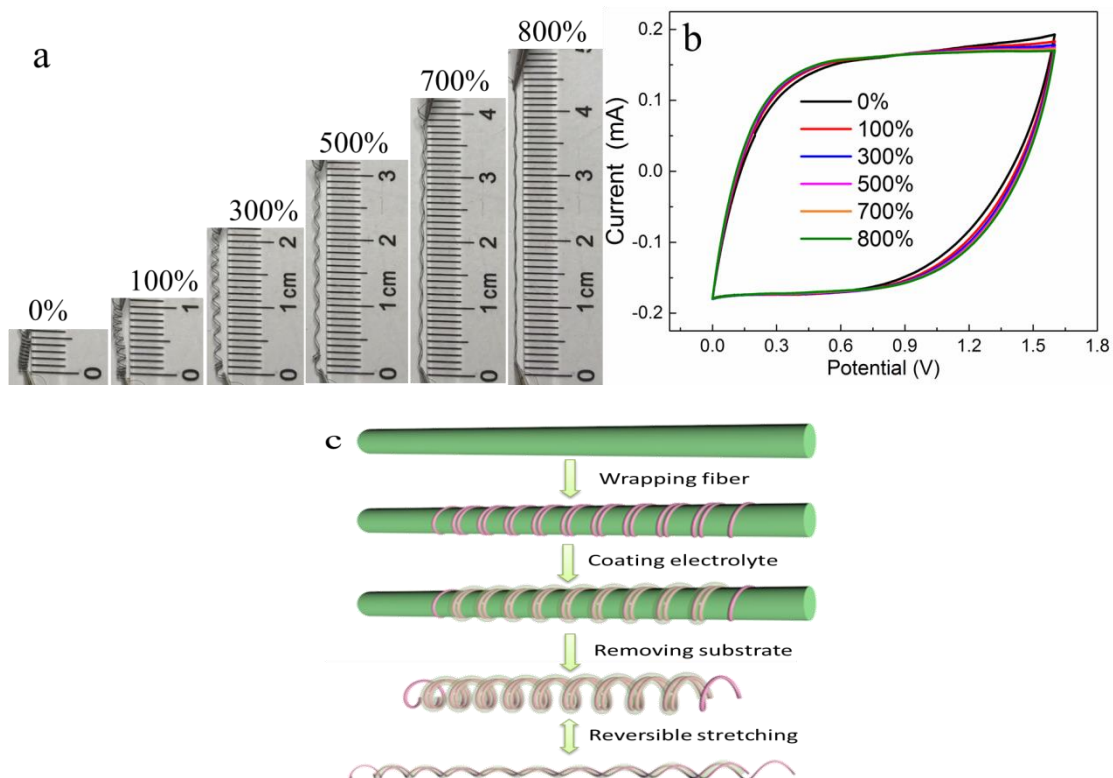


Figure S18. (a) Photograph of a SFSS being stretched to 800%. (b) CV curves at increasing strains from 0% to 800%. (c) Schematic illustration to the fabrication of PEDOT-S:PSS-based SFSS.

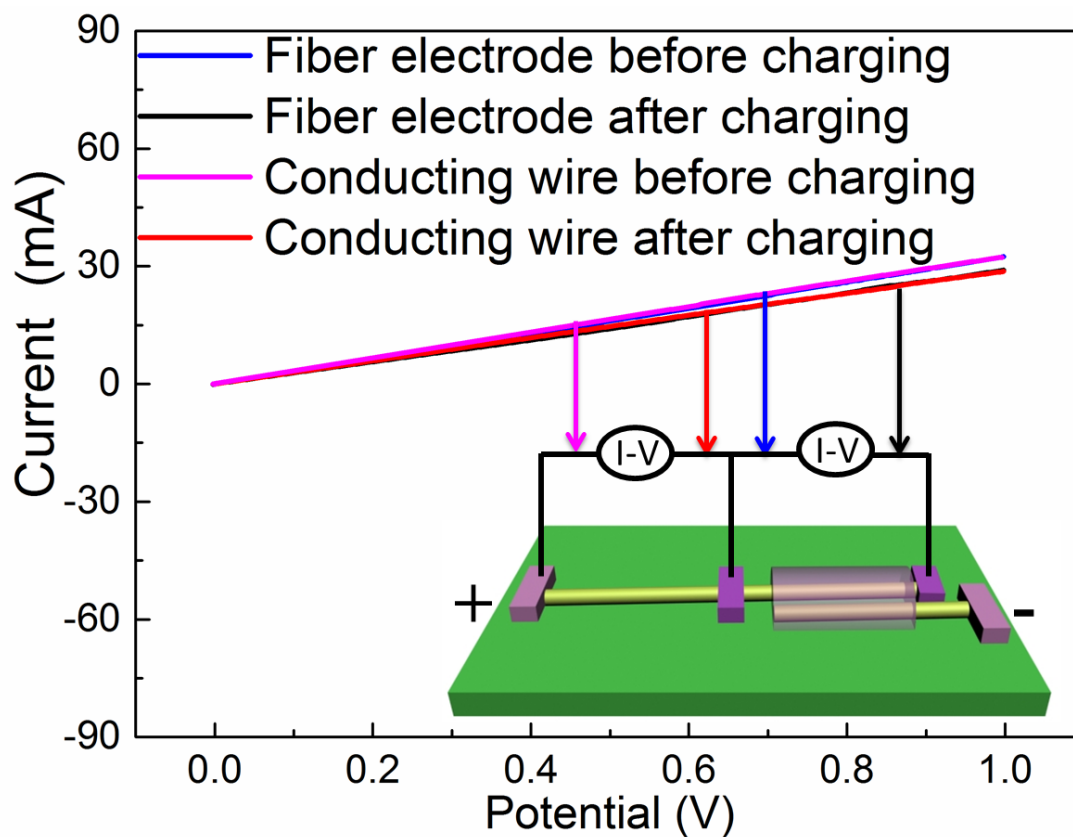


Figure S19. Current-potential (I-V) curves of PEDOT-S:PSS fiber before and after charging as the conducting wire and electrode of energy storage device.

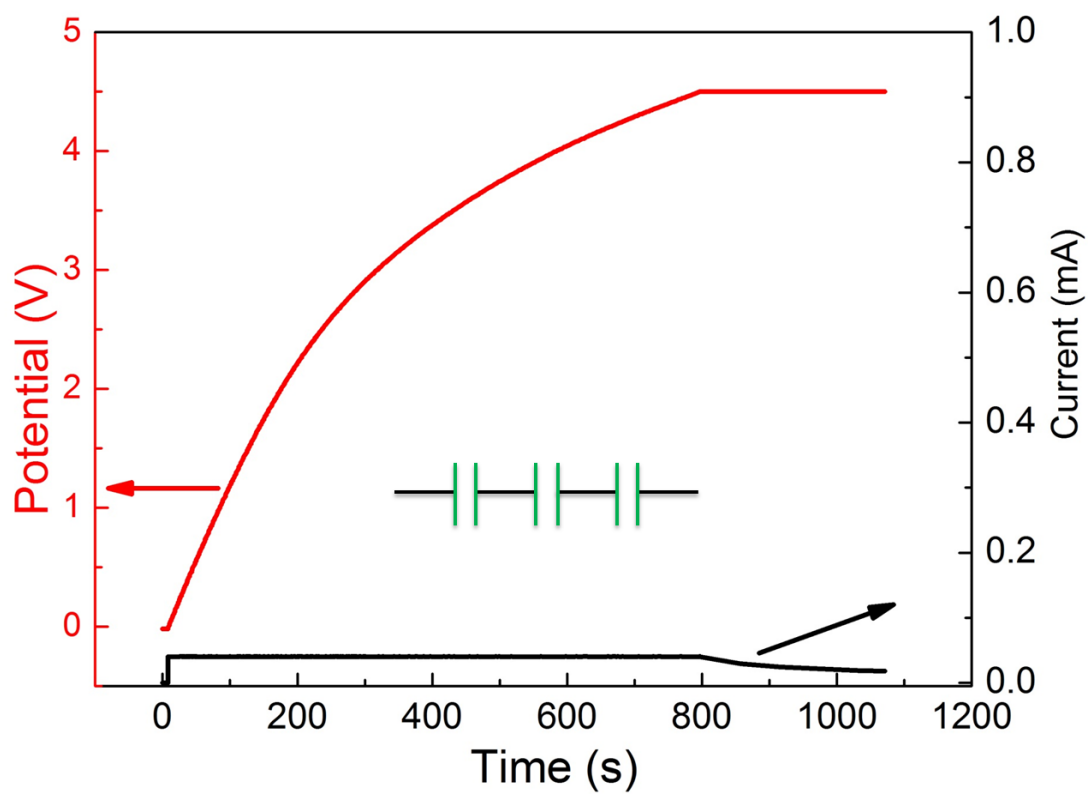


Figure S20. Charge curves of T-SFSSs with the twisted PEDOT-S:PSS electrodes.

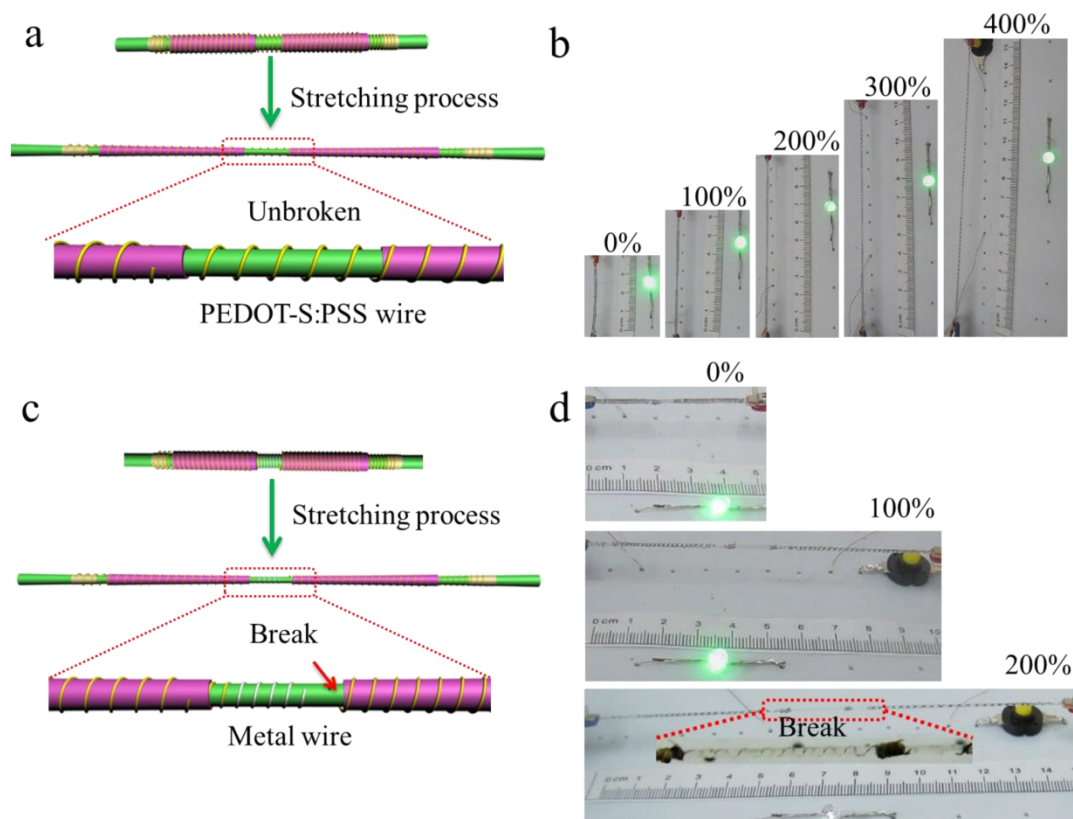


Figure S21. The comparison between (a, b) the T-SFSSs and (c, d) the traditional stretchable supercapacitor assemblies. The T-SFSSs are built by connecting two SFSSs electrically in series without the use of additional metal wires for connection. Each SFSS is electrically connected in series by using the all-in-one fibers serve as both conductive wire for electrical connection and electrode for energy storage. The traditional stretchable supercapacitor assemblies are consisting of two SFSSs in series connected by spring-like Ti wires. The T-SFSSs can be stretched up to 400%. However, the traditional stretchable supercapacitors broke at the welding point upon stretching to 200%.

3. Supporting tables

Table S1. Summary of diameter, electrical and mechanical properties of PEDOT:PSS fibers under different treating conditions.

Sample	Time /s			Diameter / μm	σ / S cm^{-1}	P/ Mpa	Strain /%
	EG	IPA	H ₂ SO ₄				
PEDOT-S:PSS-#1 (PEDOT:PSS)	10	10	/	71.0	19.8	74.1	6
PEDOT-S:PSS-#2	10	10	30	64.6	248.2	82.8	12
PEDOT-S:PSS-#3	10	10	60	61.9	394.6	85.8	13
PEDOT-S:PSS-#4	10	10	180	57.9	559.9	97.7	21
PEDOT-S:PSS-#5	10	10	300	51.2	1106.5	112.7	23
PEDOT-S:PSS-#6	10	10	600	44.0	1771.8	97.0	13
PEDOT-S:PSS-#7	/	10	600	57.1	582.1	61.1	12
PEDOT-S:PSS-#8	10	/	600	65.2	423.1	53.3	17

Table S2. The electrical properties of PEDOT-S:PSS#6 at different length

Samples	Diameter/ μm	Resistance/ Ω	Electrical conductivity/ S cm^{-1}	Average resistance/ $\Omega \text{ cm}^{-1}$	Average conductivity/ S cm^{-1}
1cm-#1	44.0	35.8	1839.7	37.3	1771.8
1cm-#2		35.0	1881.7		
2cm-#1		77.9	1690.9		
2cm-#2		75.6	1742.3		
3cm-#1		110.4	1790.2		
3cm-#2		118.4	1668.9		
4cm-#1		146.2	1801.9		
4cm-#2		156.6	1682.2		
5cm-#1		186.8	1762.9		
5cm-#2		177.3	1857.6		

Table S3. Overall specific capacitance of T-SFSSs with 1, 2, 4 and 8 cells in both theoretical and experimental aspects.

	1 cell	2 cells	4 cells	8 cells
Theoretical specific capacitance	56.4 mF cm ⁻²	28.2 mF cm ⁻²	14.1 mF cm ⁻²	7.1 mF cm ⁻²
Experimental specific capacitance	56.4 mF cm ⁻²	27.5 mF cm ⁻²	14.8 mF cm ⁻²	7.2 mF cm ⁻²
Experimental energy density	5.0 μW h cm ⁻² /2.2 mW h cm ⁻³	9.8 μW h cm ⁻² /4.3 mW h cm ⁻³	21.0 μW h cm ⁻² /9.3 mW h cm ⁻³	41.1 μW h cm ⁻² /18.3 mW h cm ⁻³
Experimental power density	440 μW cm ⁻² /195.6 mW cm ⁻³	880 μW cm ⁻² /391.1 mW cm ⁻³	1760 μW cm ⁻² /782.2 mW cm ⁻³	3520 μW cm ⁻² /1564.5 mW cm ⁻³

The theoretical total specific capacitance of the tandem supercapacitor is

$$\frac{1}{C_{\text{total}}} = \frac{1}{C_{\text{cell}}} + \frac{1}{C_{\text{cell}}} + \dots + \frac{1}{C_{\text{cell}}}$$

$$C_{\text{total}} = \frac{C_{\text{cell}}}{n}$$

The experimental total specific capacitance of the tandem supercapacitor is

$$C_{\text{total}} = Q_{\text{tandem}} / (U_{\text{tandem}} \times 2nX) = I \times t / (U \times 2nX)$$

where X is the surface area or volume of the single electrode.

The total energy density of the tandem supercapacitor is

$$E = 0.5 \times C_{\text{Total}} \times U^2$$

$$\text{Power density: } P_V = E/t$$

where t is discharge time from GCD curves.

Table S4. Overall ESR of T-SFSSs with 1, 2, 4 and 8 cells in both theoretical and experimental aspects.

	1 cell	2 cells	4 cells	8 cells
Theoretical				
ESR(Ω)	227.3	454.6	909.2	1818.4
Experimental				
ESR(Ω)	227.3	435.6	739.7	1757.8

Table S5. Comparison of the stretchable properties of the crystalline PEDOT fiber electrodes with the previously reported stretchable fiber-shaped supercapacitors.

Electrode material	E_A ($\mu\text{W h cm}^{-2}$)	E_V (mWh cm^{-3})	Stretchability of one cell (potential window)	Stretchability of tandem multiple cells (potential window)
This work	41.1 At 1mAcm^{-2} (12.8V)	18.3 (12.8V)	800% (1 cell, 1.6V)	400% (12.8V, tandem SFSS groups consisting of 8 cells)
PEDOT:PSS hydrogels[1]	None	None	None (0.8V)	None
CNT/PEDOT-PSS[2]	None	None	350% (0.8V)	None
PEDOT:PSS/CNF/CF[3]	None	None	100% (0.8V)	None
MoS ₂ @CNTF//MnO ₂ @PEDOT :PSS@OCNTF[4]	125.4	None	100% (1.8V)	None
PPy@CNT [5]	None	None	1000% (0.6V)	None
MnO ₂ @CNT//CNT@PPy[6]	18.88	None	30% (1.5 V)	None
CNT@PANI[7]	None	None	400% (1.0 V)	None
CNT/PANI sheet[8]	None	None	100% (1.0 V)	None
N-CNT/PU[9]	2.16	None	500% (1V)	None
GF@3D-G[10]	0.04-0.17	None	200% (0.8V)	None
CNT/MoS ₂ sheet[11]	None	1.05	240% (0.8V)	None
PPy@CNTs@urethane[12]	6.13	0.4678	130% (0.8V)	None
CNT/PPy[13]	None	None	150% (1V, substrate-free)	None
CNT@graphene@MnO ₂ [14]	None	3.37	850% (0.8V)	None
PANI@Au15@CNT[15]	None	None	400% (0.8 V)	None
PANI@Au@CNT[16]	None	None	400% (0.75V)	None
CNTs/Ag-DCYs[17]	None	4.17	150% (2.5 V)	None

MnO ₂ /CNT hybrid[18]	None	None	800% (0.8 V)	None
GWF+PANI[19]	None	None	30% (0.5 V)	None
CNT@MnO ₂ [20]	None	None	150% (0.8 V)	None
PANI/graphene[21]	None	None	30% (0.8 V)	None

E_A: Areal energy density E_V: Volumetric energy density

5. Supporting Notes

Calculation of electrical conductivity

The electrical conductivity of PEDOT-S: PSS fiber was calculated by $\sigma = l/(R \times S)$, where σ , l , R and S are the electrical conductivity, length, electrical resistance and cross-section area of PEDOT-S:PSS fiber, respectively. The electrical resistance of PEDOT-S:PSS fiber was calculated by the slope of I-V curves, which was tested by linear sweep voltammetry (LSV) method in the range of 0-1 V at the a scan rate of 5 mV s⁻¹ using a VSP-300 (Bio-Logic SAS, France) electrochemical workstation. The length of all samples was 1 cm.

Calculation of specific capacitance

The capacitance (C_{cell}) of an entire fiber supercapacitor (SC) was calculated by

$$C_{cell} = Q/U = I \times t/U$$

where Q , U , I and t are the storage charge, voltage between two electrodes, discharge current and discharge time, respectively. For a symmetric supercapacitor, the capacitance of the single electrode (C) is double of that of the entire fiber SC (C_{cell}), the capacitance of single fiber (C) was used and calculated by

$$C = 2 \times C_{cell} = 2 \times I \times t/U$$

The specific capacitance (C_X) of single fiber was calculated by

$$C_X = C/X = 2C_{cell}/X$$

where X could be surface area (A) or volume (V) for area-specific capacitance (C_A) and volume-specific capacitance (C_V), respectively. The surface area of fiber electrode

was calculated by $A = \pi \times D \times L$. The volume of fiber electrode was calculated by $V = \pi/4 \times D^2 \times L$, where D is the diameter of the fiber electrode, L is the length of the overlapped portion of the two electrodes wrapped by the electrolyte. The specific capacitance was calculated on the basis of single fiber electrode except as otherwise noted.

The practical energy (E) and power (P) of supercapacitor could be obtained from $E = 0.5 \times C \times U^2$ and $P = E/t$.

For the entire supercapacitor (based on two active fiber electrodes, without including the gel electrolyte): the areal energy density (E_A), volumetric energy density (E_V), areal power density (P_A) and volumetric power density (P_V) were calculated by

$$E_A = E/(2 \times A) = 0.5 \times C_{cell} \times U^2 / (2 \times A) = 0.125 \times (2 \times C/A) \times U^2 = 0.125 \times C_A \times U^2,$$

$$E_V = 0.125 \times C_V \times U^2$$

$$P_A = E_A/t$$

Supporting References

- [1] B. Yao; H. Wang; Q. Zhou; M. Wu; M. Zhang; C. Li; G. Shi. *Adv. Mater.*, (2017) 10.1002/adma.201700974.
- [2] T. Chen; R. Hao; H. Peng; L. Dai. *Angew. Chem. Int. Ed.*, 54 (2015) 618-622.
- [3] K. Dong; Y. C. Wang; J. Deng; Y. Dai; S. L. Zhang; H. Zou; B. Gu; B. Sun; Z. L. Wang. *ACS nano*, 11 (2017) 9490-9499.
- [4] Q. Zhang; J. Sun; Z. Pan; J. Zhang; J. Zhao; X. Wang; C. Zhang; Y. Yao; W. Lu; Q. Li; Y. Zhang; Z. Zhang. *Nano Energy*, 39 (2017) 219-228.
- [5] Y. Huang; M. Zhong; F. Shi; X. Liu; Z. Tang; Y. Wang; Y. Huang; H. Hou; X. Xie; C. Zhi. *Angew. Chem. Int. Ed.*, 56 (2017) 9141-9145.
- [6] J. Yu; W. Lu; J. P. Smith; K. S. Booksh; L. Meng; Y. Huang; Q. Li; J.-H. Byun; Y. Oh; Y. Yan; T.-W. Chou. *Adv. Energy Mater.*, 7 (2017) 1600976.
- [7] Z. Zhao; J. Tian; Y. Sang; A. Cabot; H. Liu. *Adv. Mater.*, 27 (2015) 2557-2582.
- [8] X. Chen; H. Lin; P. Chen; G. Guan; J. Deng; H. Peng. *Adv. Mater.*, 26 (2014) 4444-4449.
- [9] Z. Zhang; L. Wang; Y. Li; Y. Wang; J. Zhang; G. Guan; Z. Pan; G. Zheng; H. Peng. *Adv. Energy Mater.*, (2016) 1601814.
- [10] Y. Meng; Y. Zhao; C. Hu; H. Cheng; Y. Hu; Z. Zhang; G. Shi; L. Qu. *Adv. Mater.*, 25 (2013) 2326-2331.
- [11] T. Lv; Y. Yao; N. Li; T. Chen. *Angew. Chem. Int. Ed.*, 55 (2016) 9191-9195.
- [12] J. Sun; Y. Huang; C. Fu; Z. Wang; Y. Huang; M. Zhu; C. Zhi; H. Hu. *Nano Energy*, 27 (2016) 230-237.

- [13] Y. Shang; C. Wang; X. He; J. Li; Q. Peng; E. Shi; R. Wang; S. Du; A. Cao; Y. Li. *Nano Energy*, 12 (2015) 401-409.
- [14] H. Wang; C. Wang; M. Jian; Q. Wang; K. Xia; Z. Yin; M. Zhang; X. Liang; Y. Zhang. *Nano Res.*, (2017) 10.1007/s12274-017-1782-1.
- [15] W. Zhu; Y. Zhang; X. Zhou; J. Xu; Z. Liu; N. Yuan; J. Ding. *Nanoscale Res. Lett.*, 12 (2017).
- [16] J. Xu; J. Ding; X. Zhou; Y. Zhang; W. Zhu; Z. Liu; S. Ge; N. Yuan; S. Fang; R. H. Baughman. *J. Power Sources*, 340 (2017) 302-308.
- [17] M. Shi; C. Yang; X. Song; J. Liu; L. Zhao; P. Zhang; L. Gao. *Chem. Eng. J.*, 322 (2017) 538-545.
- [18] C. Choi; J. H. Kim; H. J. Sim; J. Di; R. H. Baughman; S. J. Kim. *Adv. Energy Mater.*, 7 (2017) 1602021.
- [19] X. Zang; M. Zhu; X. Li; X. Li; Z. Zhen; J. Lao; K. Wang; F. Kang; B. Wei; H. Zhu. *Nano Energy*, 15 (2015) 83-91.
- [20] Q. Tang; M. Chen; G. Wang; H. Bao; P. Saha. *J. Power Sources*, 284 (2015) 400-408.
- [21] Y. Xie; Y. Liu; Y. Zhao; Y. H. Tsang; S. P. Lau; H. Huang; Y. Chai. *J. Mater. Chem. A*, 2 (2014) 9142-9149.